# Airfoil in a Contracting or Diverging Stream

B. LAKSHMINARAYANA* and M. T. WHITE†
*Pennsylvania State University, University Park, Pa.*

**A theoretical and experimental investigation of the flow around an airfoil in a contracting or diverging stream is carried out in this paper. An expression for the vortex distribution, which satisfies the kinematic condition on the airfoil surface and the Kutta condition at the trailing edge, is derived. The predicted values of the lift and the surface pressure distribution, at various values of incidences and mean flow acceleration, agrees very well with the measured values. In converging flow, the circulation and lift are found to increase with increase in velocity ratio (ratio of outlet to inlet velocity). Considerable change in airfoil pressure distribution is observed, its effect being dominant on the suction surface. With diverging mean flow, both circulation and lift decrease with decrease in velocity ratio. The decrease in mean velocity seems to have dominant effect on the pressure surface. Finally, the theoretical and experimental investigation seems to indicate that the ratio of lift coefficients, with and without change in mean flow, can be expressed as $C_L/C_{L2d} = VR$, where $VR$ = velocity ratio.**

## Nomenclature

$A_0, A_1, \ldots, A_n$ = Fourier coefficients [Eq. (11)]
$B, D, E$ = functions of $\theta$ [Eqs. (13–15)]
$C$ = chord length
$C_L$ = lift coefficient (nondimensionalized with respect to inlet dynamic head)
$C_l$ = loading coefficient (nondimensionalized with respect to inlet dynamic head)
$C_p$ = static pressure coefficient (nondimensionalized with respect to inlet dynamic head) [Eq. (30)]
$h$ = width of the channel (Fig. 1)
$K$ = $dh/h_1dx$
$L$ = lift
$l$ = loading [Eq. (26)]
$p$ = static pressure
$U$ = mean velocity in the absence of the airfoil
$u', v'$ = velocity perturbations due to airfoil camber
$u''$ = velocity perturbations due to thickness
$VR$ = velocity ratio $U_2/U_1$
$x, y, z$ = coordinates (Fig. 1)
$\alpha$ = angle of incidence
$\Gamma$ = total circulation around the airfoil
$\gamma$ = strength of the vortex sheet
$\eta$ = camber function

*Subscripts*

1 = values at leading edge
2 = values at trailing edge
$2d$ = two-dimensional ($K = 0$)
$-$ = suction surface
$+$ = pressure surface
$l$ = local values

## I. Introduction

THE influence of boundaries on the fluid motion around airfoil or airfoil system is of great practical importance in aerodynamics. The investigations carried out hitherto are confined to walls parallel to the original motion. In this case, the mean velocity past the airfoil remains constant. In several applications, where accelerating or decelerating mean flow is encountered, the mean velocity or the so called free-stream velocity, which is the undisturbed velocity in the absence of the airfoil, cannot be considered constant along the airfoil chord and it is essential to allow for its variation. One of the common examples is when the neighboring surfaces of the body (such as fuselage and wing nacelle) accelerate or decelerate the mean flow through the wing. Furthermore, the boundary-layer growth along the end walls of a wind tunnel or water tunnel, in which a wing is tested, a change in mean velocity occurs and the aerodynamics or hydrodynamics of the wing is appreciably changed. Other applications where the change of mean flow velocity is encountered is in the flow through compressor, propeller, pump or fan with diverging or converging hub and annulus walls. Most of the modern day compressors and fans have appreciable change in axial velocity (10 to 20%).

Whereas the results of wing theory are widely used in propeller (both shrouded and unshrouded) and fan design, the compressor design is largely based on cascade flow theories. Hence, an investigation of the effects of change in mean velocity is of considerable interest to not only the wing aerodynamicist, but also to compressor, fan and propeller designers. Furthermore, the development on airfoil theory (allowing for change in mean velocity) is a first step in the solution of cascade flow where the axial and mean velocities are changing through the passage. Some advances have been made in predicting the effect of axial velocity change through a cascade by Shaalan and Horlock,[1] and Mani and Acosta.[2] All these methods are numerical and considerable discrepancy between theoretical and experimental results has been reported (Ref. 4). The investigations reported here should help in the development of an adequate cascade theory allowing for axial velocity change.

In this paper, a theoretical and experimental investigation of the flow around an airfoil in a contracting or diverging stream is carried out. An expression for the vortex distribution, which satisfies the kinematic condition on the wing surface and the Kutta condition at the trailing edge, is derived. The theory is valid for small variations in mean velocity ($\pm 25\%$ of the inlet velocity). The predicted values of total lift and the local pressure distribution agree very well with the experimental measured values. The experimental investigation is carried out in a wind tunnel with sloping side walls to obtain chordwise variation in mean velocity. The gap between the side walls is varied linearly.

Received October 8, 1971; revision received January 12, 1972. The experimental investigation reported in this paper was carried out at the Ordnance Research Laboratory of The Pennsylvania State University. The authors wish to acknowledge the assistance of John R. Ross in the experimental investigation.

Index categories: Airplane and Component Aerodynamics; Propulsion System Hydrodynamics; Subsonic and Supersonic Airbreathing Propulsion.

* Associate Professor, Department of Aerospace Engineering, Associate Fellow AIAA.

† Student, Department of Aerospace Engineering.

## II. Theoretical Development

The aerodynamics of a wing spanning a slightly converging or diverging channel is investigated here. The variation of the channel width is assumed to be linear and the length of the contracting or diverging section is assumed to be the same as airfoil chord. The experimental results presented later indicate that the theory is valid up to about $\pm 25\%$ variation in mean velocity (about its value at the leading edge), which covers the majority of the flows encountered in practice. The mean flow is assumed to be inviscid, steady and incompressible, but nonuniform in the $x$ direction (Fig. 1). For simplicity, a linear contraction or divergence is assumed, but the theory can be extended to other types of variation of the channel width. The theory assumes that spanwise flows are zero, which is valid exactly at the plane of symmetry (midspan). The experimental results show that the theory is valid at most of the spanwise positions, except near the channel walls.

Referring to Fig. 1, if $U_1$ and $h_1$ are velocity and channel width respectively at inlet,

$$U_1 = [1 + (1/h_1)(dh/dx)x]U \tag{1}$$

where $U$ is the local mean velocity and

$$(1/h_1)/(dh/dx) = K = \text{a const} \tag{2}$$

Thus,

$$dU/dx = -UK/(1 + Kx) = -U_1K/(1 + Kx)^2 \tag{3}$$

The continuity equation valid near the plane of symmetry is,

$$\partial(uh)/\partial x + \partial(vh)/\partial y = 0 \tag{4}$$

where

$$u = U(x) + u'(x) \tag{5}$$

$$v = V(x) + v'(x) \tag{6}$$

$u'$, $v'$ are perturbations in velocity due to airfoil in the contracting or diverging stream.

Knowing that

$$dU/dx = -(U/h)(dh/dx)$$

Eq. (4) can be expressed as

$$-(u'/U)(dU/dx) + \partial u'/\partial x + \partial v'/\partial y = 0 \tag{7}$$

If the perturbation in velocity produced by the contraction is the same order as those produced by the airfoil, and if these perturbations are small compared to $U$, then the first term in Eq. (7) can be neglected. Furthermore, the flow is irrotational. Thus the perturbation potential satisfies the two-dimensional equations. These approximations are in the theoretical development, but the change in local mean velocities is taken into account in calculating the perturbations produced by the airfoil. Furthermore, Wilson et al.[3] have proved that the blade thickness has negligible effect in changing the aerodynamic characteristics of a cascade of blades with mean velocity change. Thus the problem on hand reduces to that of finding the effect of mean velocity change on the circulation distribution.

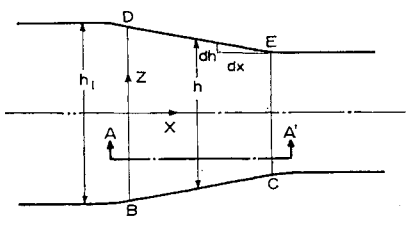


**Fig. 1 Configuration and notation.**

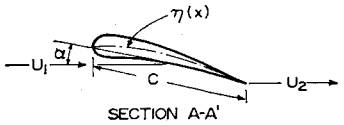


### Vortex Distribution

Using the thin airfoil approximation, the vortex distribution along the airfoil chord can be determined from the kinematic condition at any point $x = x_0$

$$\left\{U\left(\alpha - \frac{d\eta}{dx}\right)\right\}_{x=x_0} = \frac{1}{2\pi}\int_0^c \frac{\gamma dx}{x_0 - x} \tag{8}$$

where $\gamma$ = vortex distribution, $\alpha$ = angle of attack, and $\eta$ = camber function.

The local velocity is given by

$$U = U_1/(1 + Kx) \simeq U_1(1 - Kx + K^2x^2) \tag{9}$$

where small order terms containing $K^3$, $K^4$, etc. are neglected. Substituting Eq. (9) and

$$x = C/2(1 - \cos\theta)$$

$$x_0 = C/2(1 - \cos\phi)$$

in Eq. (8), the Kinematic condition reduces to

$$U_1\left[1 - \frac{KC}{2}(1 - \cos\phi) + \frac{K^2C^2}{4}(1 - \cos\phi)^2\right]\left(\alpha - \frac{d\eta}{dx}\right)_{x=x_0} = \frac{1}{2\pi}\int_0^\pi \frac{\gamma(\theta)\sin\theta d\theta}{\cos\theta - \cos\phi} \tag{10}$$

Let us write

$$\frac{d\eta}{dx}(\theta) = \alpha - A_0 + \sum_1^\infty A_n \cos n\theta \tag{11}$$

The solution of integral Eq. (10) is then given by‡

$$\gamma(\theta) = 2U_1\left\{A_0\frac{1 + \cos\theta}{\sin\theta}\left(1 - \frac{KC}{2}B + \frac{K^2C^2}{4}D\right) + \sum_1^\infty (A_n \sin n\theta)\left[1 - \frac{KC}{2}E + \left(\frac{KCE}{2}\right)^2\right]\right\} \tag{12}$$

where

$$B = 1 + \frac{\sin^2\theta}{1 + \cos\theta} \tag{13}$$

$$D = \frac{3}{2} + \frac{2\sin^2\theta}{1 + \cos\theta} - \frac{\sin 2\theta \sin\theta}{2(1 + \cos\theta)} \tag{14}$$

$$E = 1 - \cos\theta \tag{15}$$

Equation (12) satisfies Eq. (10) [with Eq. (11)] exactly and the Fourier coefficients $A_0, A_1, \ldots, A_n$ are functions of airfoil geometry only, as in a plane flow ($K = 0$). Furthermore, the $\gamma$ distribution satisfies the Kutta condition: $\gamma(\pi) = 0$. It should be remarked here that the $\gamma$ distribution given by Eq. (12) consists of basic distribution for plane flow ($K = 0$), superposed on this distribution is the effect of change in mean velocity.

The values of $\gamma/\gamma_{2d}$, where $\gamma_{2d}$ is the vortex strength for plane flow with $KC = 0$, derived from Eq. (12) for a flat plate

‡ The definite integrals appearing in this equation can be solved by well-known Glauert's integral. For example

$$\int_0^\pi E^2 \frac{\sin n\theta \sin\theta}{\cos\theta - \cos\phi} = -\pi \cos n\phi(1 - \cos\phi)^2$$

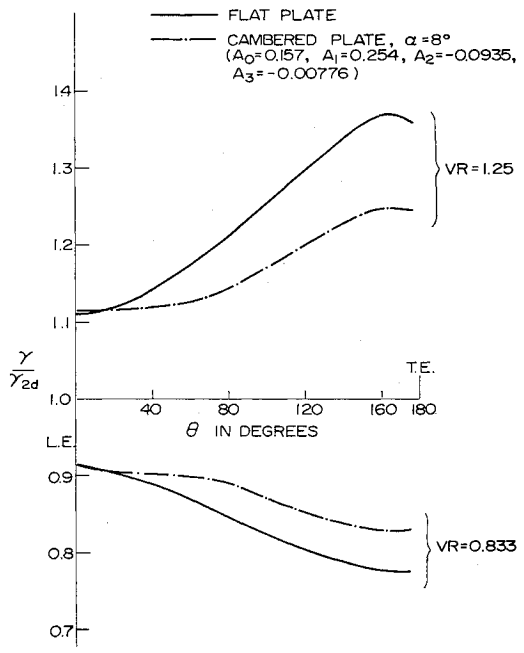


**Fig. 2 Vortex distribution for a flat plate and cambered airfoil in diverging and converging flow (theoretical).**

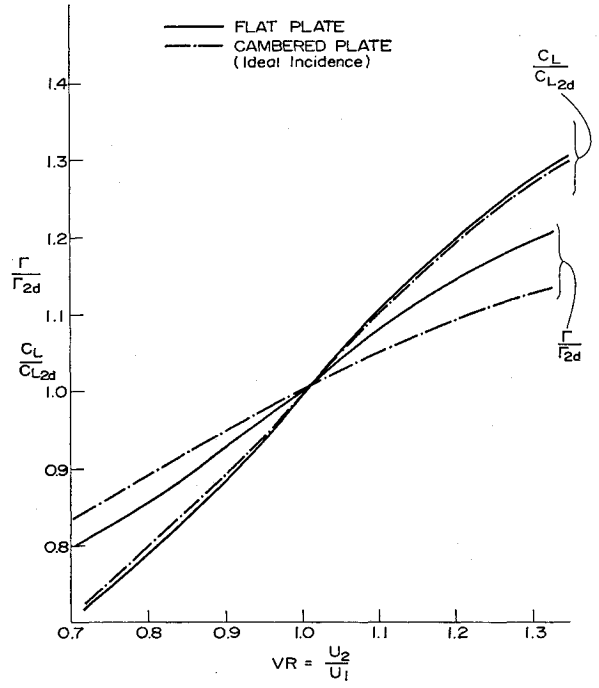


**Fig. 3 Variation of circulation and lift coefficient with velocity ratio (theoretical).**

at incidence and cambered airfoil§ at $\alpha = 8°$ and at $VR = 1.25$ and 0.833 are plotted in Fig. 2. The velocity ratio $VR$ is given by

$$VR = U_2/U_1 = 1/(1 + KC) \tag{16}$$

The ratio $\gamma/\gamma_{2d}$ increases continuously towards the trailing edge of the airfoil for both these cases, when the mean velocity ($U$) is increasing. The circulation increases across the entire blade chord for an accelerating flow and decreases for a decelerating mean flow. Change in mean velocity seems to have a larger effect for a flat plate at incidence as compared to a cambered plate. Even at the leading edge, appreciable change in $\gamma$ is observed for both cases (Fig. 2).

### Circulation

Total circulation around the airfoil is given by

$$\Gamma = \int_0^c \gamma dx$$

Substituting Eq. (12) in the above expression and integrating, the following expression results

$$\frac{2\Gamma}{\pi U_1 C} = (2A_0 + A_1) + \frac{KC}{2}\left(-3A_0 - A_1 + \frac{A_2}{2}\right) + \frac{K^2C^2}{4}\left(5A_0 + A_1 - A_2 + \frac{A_3}{4}\right) \tag{17}$$

The circulation in two-dimensional flow ($KC = 0$) is given by

$$\Gamma_{2d} = \frac{\pi U_1 C(2A_0 + A_1)}{2} \tag{18}$$

The ratio of circulation with and without change in mean velocity is

$$\frac{\Gamma}{\Gamma_{2d}} = 1 - \frac{(KC/2)[3A_0 + A_1 - (A_2/2)] - [(K^2C^2)/4][5A_0 + A_1 - A_2 + (A_3/4)]}{(2A_0 + A_1)} \tag{19}$$

§ The camber of the airfoil used as a test case in Fig. 2 is the same as that used for experimental investigation (Sec. III). The camber is given by Eq. (11) with $A_0 = 0.157$, $A_1 = 0.254$, $A_2 = -0.0935$, $A_3 = -0.00776$.

The ratio of total circulation ($\Gamma/\Gamma_{2d}$), with and without change in mean velocity, is plotted in Fig. 3 at various velocity ratios ($VR$) for a) a flat plate airfoil at incidence b) a circular arc cambered airfoil at ideal incidence ($A_0 = A_2 = A_3 \cdots = 0$). It is evident that the total circulation varies almost linearly with $VR$ for both flat plate and cambered airfoils. In both cases, the circulation increases with accelerating flow and decreases with decelerating flow.

### Lift Coefficient

The lift of an airfoil in a contracting or diverging stream is

$$L = \int_0^c \rho U(x)\gamma dx \tag{20}$$

The corresponding expression for two-dimensional case is

$$L_{2d} = \rho U_1 \int_0^c \gamma dx$$

Hence the ratio of lift coefficients is

$$\frac{C_L}{C_{L_{2d}}} = \int_0^c \frac{U(x)}{U_1}\gamma dx \Big/ \Gamma_{2d} \tag{21}$$

where $C_L$ and $C_{L_{2d}}$ are normalized with respect to the same inlet dynamic pressure.

Substitution of Eq. (12) and (9) in Eq. (21) results in the following expression

$$\frac{C_L}{C_{L_{2d}}} = \frac{CU_1}{\Gamma_{2d}}\int_0^\pi \left\{1 - \frac{KC}{2}E + \left(\frac{KCE}{2}\right)^2\right\} \times \left\{A_0\frac{1+\cos\theta}{\sin\theta}\left(1 - \frac{KC}{2}B + \frac{K^2C^2}{4}D\right) + \sum_1^\infty A_n(\sin n\theta) \times \left[1 - \frac{KCE}{2} + \left(\frac{KCE}{2}\right)^2\right]\right\}\sin\theta d\theta \tag{22}$$

The above equation can be integrated to give (neglecting small-order terms such as $K^3$, $K^4$, etc.),

$$\frac{C_L}{C_{L_{2d}}} = 1 - \frac{KC[2A_0 + A_1 - (A_2/2)] - (K^2C^2/4)(3A_1 - 3A_2 + (A_3/2) + 7A_0)}{2A_0 + A_1} \quad (23)$$

The ratio of lift coefficients for a flat plate airfoil is given by

$$C_L/C_{L_{2d}} = 1 - KC + (7/8)K^2C^2 \quad (24)$$

The corresponding expression for a circular cambered airfoil at ideal incidence is

$$C_L/C_{L_{2d}} = 1 - KC + (3/4)K^2C^2 \quad (25)$$

The results derived from Eqs. (24) and (25) are plotted in Fig. 3. The lift coefficient increases in a converging mean flow and decreases in a diverging mean flow.

#### Loading Coefficient

The change in local loading due to varying mean flow is given by,

$$\Delta l = l - l_{2d} = \rho U(x)\gamma - \rho U_1\gamma_{2d} \quad (26)$$

Substituting for $U$ from Eq. (9) and $\gamma$ from Eq. (12), and after some simplification Eq. (26) can be expressed as (neglecting small order terms $K^3$, $K^4$, ..., etc.)

$$\Delta C_l = \frac{\Delta l}{\frac{1}{2}\rho U_1^2} = 2(3K^2x^2 - 2Kx)\frac{\gamma_{2d}}{U_1} + 4A_0\left(\frac{C-x}{x}\right)^{1/2} \times \left[\frac{-KC}{2} + K^2x^2\left(\frac{2x}{C} + \frac{5}{4}\frac{C}{x}\right)\right] \quad (27)$$

where $\Delta C_l$ is the change in loading coefficient and

$$\frac{2\gamma_{2d}}{U_1} = C_{l_{2d}} = [C_p(x, 0_-) - C_p(x, 0_+)]_{2d} \quad (28)$$

$C_p$ = static pressure coefficient on the airfoil surface.

It is clear from the preceding expression [Eq. (27)] that the change in loading coefficient (based on inlet dynamic pressure) increases continuously towards the trailing edge for converging flows ($K$ being negative) and vice versa for diverging flows ($K$ being positive).

It is interesting to note that the use of simplified expression given above involves only the knowledge of $C_{l_{2d}}$, $A_0$ and $K$.

#### Pressure Distribution

The pressure distribution on the airfoil is given by

$$p_1 + \tfrac{1}{2}\rho U_1^2 = p_l + \tfrac{1}{2}\rho(U \pm u' + u'')^2 \quad (29)$$

where $u'$ = perturbation due to $\gamma$, and $u''$ = perturbation due to source and sink (thickness effect).

Using thin airfoil theory approximations and assuming that the thickness effects are the same as that of plane flow, the following expression for static pressure coefficient can be derived

$$C_p = \frac{p_l - p_1}{\frac{1}{2}\rho U_1^2} = 1 - \left(\frac{U}{U_1}\right)^2 + \frac{U}{U_1}C_{p_{2d}} - \frac{U}{U_1}\left(\frac{\gamma(\theta) - \gamma(\theta)_{2d}}{U_1}\right) \quad (30)$$

where $C_{p_{2d}}$ = pressure coefficient in plane flow ($K = 0$).

Substituting Eq. (9) for $U/U_1$ and Eq. (12) for $\gamma(\theta)$ in Eq. (30), the static pressure coefficient can be expressed as (neglecting small order terms such as $K^3$, $K^4$, etc.),

$$C_p = (2Kx - 3K^2x^2) + (1 - Kx + K^2x^2)\left\{C_{p_{2d}} - 2A_0\frac{1+\cos\theta}{\sin\theta} \times \left(-\frac{KC}{2}B + \frac{K^2C^2}{4}D\right) - 2\sum_1^\infty (A_n \sin n\theta)\left[-\frac{KCE}{2} + \left(\frac{KCE}{2}\right)^2\right]\right\} \quad (31)$$

where $B$, $D$ and $E$ are given by Eqs. (13–15).

The pressure coefficient on the airfoil surface (on both pressure and suction surface) can be computed from the previous equation from known values of $C_{p_{2d}}$, $K$ and Fourier coefficients $A_0, A_1, \ldots, A_n$.

The first two terms in Eq. (30) and the first term in Eq. (31) corresponds to direct change (in the absence of airfoil) in $C_p$ distribution in the flow due to changing mean flow. Whereas, the remaining terms represent the change in perturbation flow due to airfoil in a converging or diverging flow.

## III. Experimental Results

The validity of the theory developed in Sec. II is verified by an experimental investigation of the flow around an airfoil in a contracting stream. These investigations were carried out with an isolated airfoil spanning the wind-tunnel sidewalls. A linear contraction, extending from leading edge to trailing edge of the airfoil was obtained by using movable sidewalls (*BC*, *DE* in Fig. 1). The movable sidewalls provide for velocity ratios (*VR*) ranging from 1.00 to 1.26. The upstream and downstream tunnel sections were straight. The leading and trailing edges of the sidewalls were faired to obtain a smooth contraction.

The NACA-65-($8A_2I_{8b}$) 10 airfoil section used is a compressor blade of "trailing loaded" type. The loading at design lift coefficient (=0.8) varies linearly over about the forward 80% of blade chord, beyond which it is essentially uniform. Detail profile and camber geometry of this airfoil is given in Ref. 5. The flow and airfoil geometry are shown in Table 1. The airfoil incorporated twelve static taps on each surface. The static pressures were measured at mid span ($z = 0$) as well as at $z = 3$ in.

The experiment was run at three different incidence angles for three velocity ratios (*VR*). The pressure distributions measured at $\alpha = 1°$, 6° and 8° and $VR = 1.0$, 1.115 and 1.26 are plotted in Figs. 4–7. It should be remarked here that the pressure coefficients in all the cases are nondimensionalized with respect to the inlet dynamic head.

It is evident from these plots (Figs. 4–7) that the change in

**Table 1 Flow and airfoil geometry**

| | |
|---|---|
| Chord length (c) | 7 in. |
| Span (leading edge) | 14.5 in. |
| Incidence | 1°, 6° and 8° |
| Velocity ratio (VR) | 1.0, 1.115, 1.26 |
| Reynolds number (based on chord length) | $\simeq 3.6 \times 10^5$ |

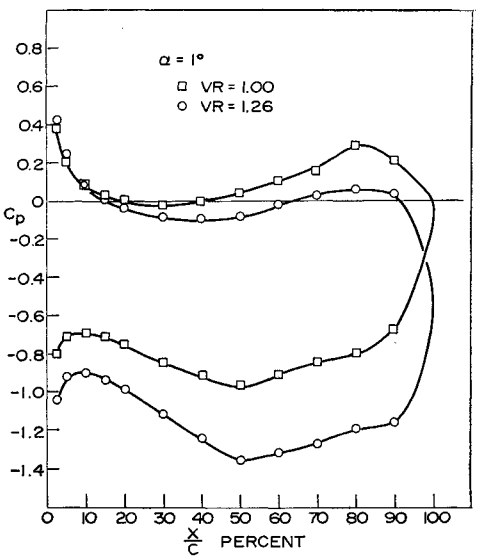


**Fig. 4 Measured airfoil pressure distribution for $\alpha = 1°$, and $VR =$ 1.00 and 1.26.**

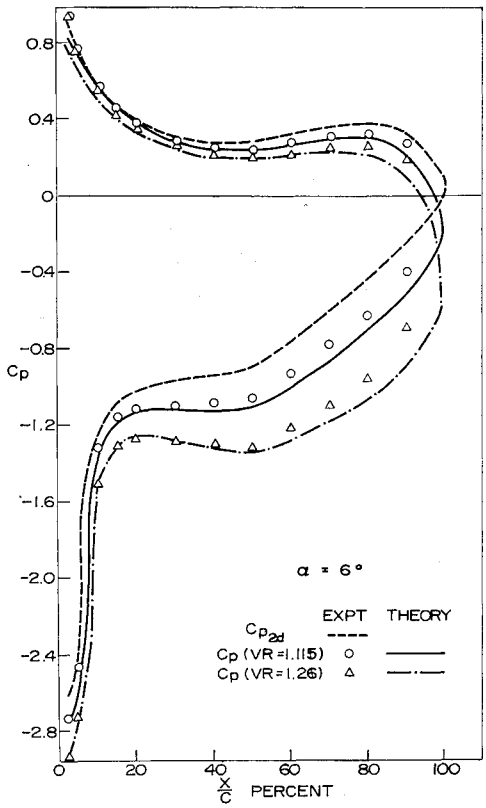


Fig. 5 Measured and predicted airfoil pressure distribution for $\alpha = 6°$, and $VR = 1.00$, 1.115 and 1.26.

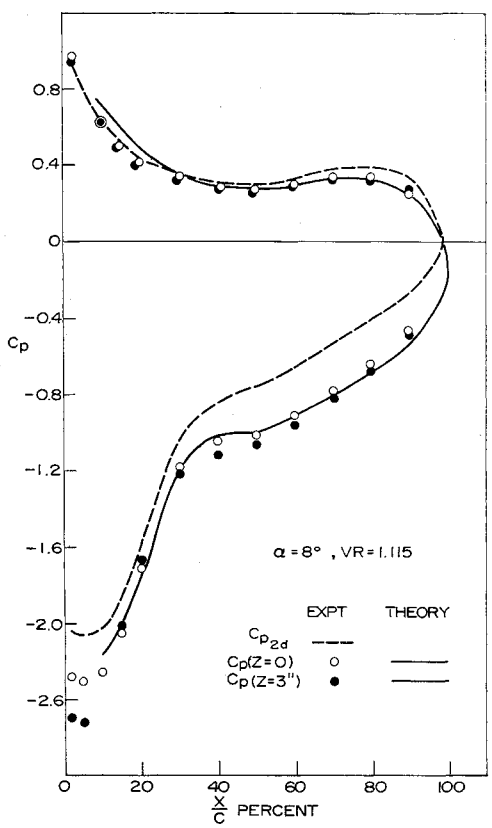


Fig. 6 Measured and predicted airfoil pressure distribution for $\alpha = 8°$, and $VR = 1.00$ and 1.115.

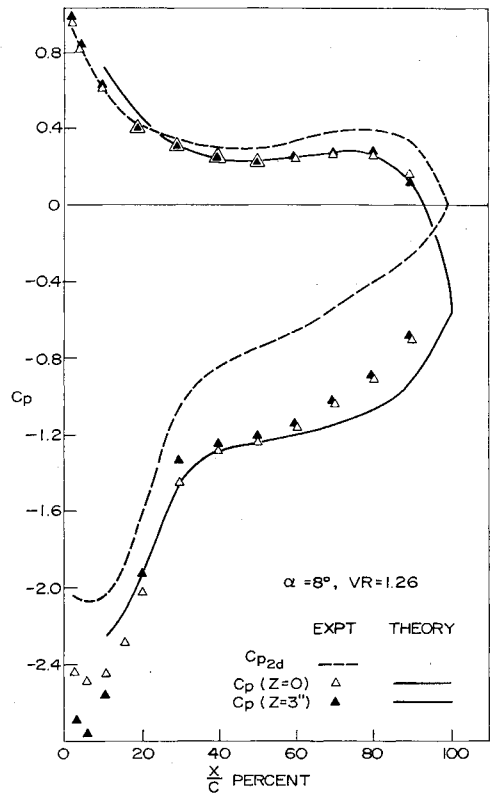


Fig. 7 Measured and predicted airfoil pressure distribution for $\alpha = 8°$, and $VR = 1.00$ and 1.26.

$VR$ substantially affects the pressure distribution, especially on the suction surface. The trend is consistent at all the incidences investigated here. The change in $C_p$ distribution for $VR \neq 1.0$ is caused by two effects: a) change in mean velocity $U(x)$ in the absence of airfoil—direct effect; and b) change in $\gamma$ distribution—indirect effect.

Both of these changes affect the pressure coefficient in Eq. (30). Equation (31) indicates that the direct effect of an increase in mean velocity (if $\gamma$ is held constant) is to increase suction pressures and decrease pressure on the pressure surface. Whereas, an increase in $\gamma$ (indirect effect) brings about an increase in both suction pressure as well as the pressure on the pressure surface. Hence, an increase in $U$ has a much more dominant effect on the suction surface, where the two effects are cumulative. Whereas, increase in $\gamma$ as well as $v$ has opposing effects on the pressure surface $C_p$ distribution (Figs. 4–7). Furthermore, the departure in pressure distribution between plane flow ($K = 0$) and the converging flow ($K$, $-ve$) progressively increases towards the trailing edge. Total lift increases continuously with increase in $VR$. It is also evident from Figs. 6 and 7 that the pressure distribution is almost identical both at mid span ($Z = 0$) and at $Z = 3$ in., thus confirming the two-dimensional flow approximations made in the theoretical development of the flow.

### Comparison with the Theoretical Predictions

In order to compare the predicted values of lift, loading and pressure distribution with the measured values, a knowledge of the Fourier coefficients $A_0, A_1, \ldots, A_n$ [Eq. (11)] is essential. These can be derived from the numerical integration of the equations (since the camber line of NACA-65-($8A_2I_{8b}$)$_{10}$ profile cannot be represented by a simple function),

$$A_0 = \alpha - \frac{1}{\pi}\int_0^\pi \frac{d\eta}{dx}(\theta)d\theta$$

$$A_n = \frac{2}{\pi}\int_0^\pi \frac{d\eta}{dx}(\theta)\cos n\theta\, d\theta$$

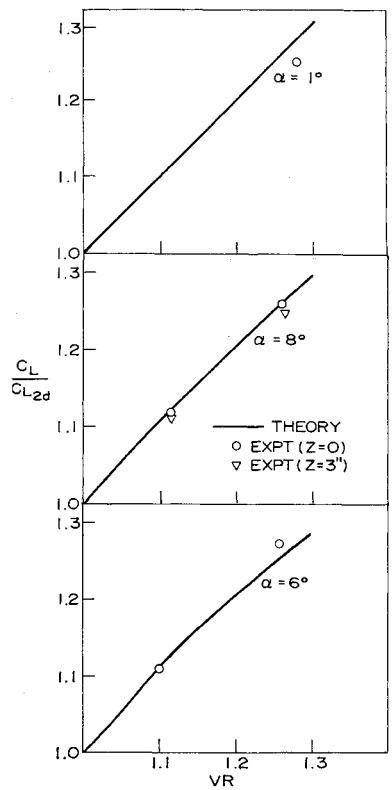


Fig. 8 Measured and predicted variation of lift coefficient with velocity ratio.

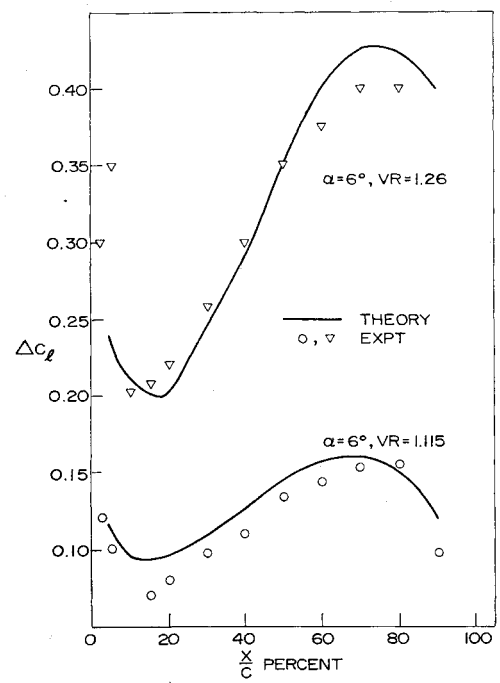


Fig. 9 Measured and predicted chordwise distribution of change in loading coefficient for $\alpha = 6°$, $VR = 1.115$ and 1.26.

The values of $d\eta/dx$ has been tabulated in Ref. 5. The values of Fourier coefficients so derived are: $A_0 = \alpha + 0.0175$, $A_1 = 0.254$, $A_2 = -0.0935$ and $A_3 = -0.00776$ etc.

The ratio of lift coefficients ($C_L/C_{L_{2d}}$) derived from Eq. (23) at various values of $VR$ are plotted in Fig. 8 and compared with the measured values. The agreement is excellent at all incidences.

It is interesting to note that the ratio $C_L/C_{L_{2d}}$ varies almost linearly with $VR$. Both experimental and theoretical investigations (Figs. 3 and 8) seem to confirm this. Furthermore, these results indicate that

$$C_L/C_{L_{2d}} \simeq VR \tag{32}$$

Even the theoretical expression [Eq. (23)] indicate that for a circular arc cambered airfoil in a slightly converging or diverging stream this ratio is

$$\frac{C_L}{C_{L_{2d}}} = 1 - KC + \frac{K^2C^2}{4}\left(\frac{3A_1 + 7A_0}{2A_0 + A_1}\right) \simeq VR$$

The change in loading coefficient ($\Delta C_l$) predicted from Eq. (27) are compared with experimental values at $\alpha = 6°$ and $VR = 1.115$ and 1.26 in Fig. 9. The agreement is good in both cases. The departure is large only near the leading and trailing edges of the airfoil. It is evident from Fig. 9 that the values of $\Delta C_l$ progressively increase towards the trailing edge.

The measured values of $C_{p_{2d}}$ (Figs. 4–7) are used in Eq. (31) in predicting the pressure distribution on the airfoil. The predicted pressure distribution on the airfoil at $\alpha = 6°$, 8° and $VR = 1.115$ and 1.26 are plotted in Figs. 5, 6, and 7. The agreement is quite good at all chordwise locations on both the surfaces of the airfoil. Appreciable departure between theory and experiment occurs only at larger $VR(=1.26)$ near the trailing edge (Figs. 5 and 7).

It is evident from these predicted and measured pressure distributions in a converging flow, the effect of increase in $U$ and $\gamma$ are cumulative on the suction side (i.e., suction pressures are increased considerably) and are opposing on the pressure side (i.e., no appreciable change in pressure on the pressure side of the airfoil). Whereas in a diverging flow, where $U$ as well as $\gamma$ decrease, these effects are cumulative on the pressure surface. Whereas, the suction pressure decreases [see Eq. (31)].

Some of these conclusions are in conformity with those of Schulze et al.,[6] who carried out experiments in a compressor rotor with converging and diverging hub wall. For $A_2/A_1$ (outlet/inlet area—diverging flow) = 1.15, the flow turning angle decreases from those of plane flow ($A_2/A_1 = 1$, $K = 0$) whereas, increased flow turning is observed in a converging case ($A_2/A_1 = 0.70$ and 0.85). In a compressor rotor, the diverging flow presents a more severe limitation on the performance due to larger pressure rise brought about by the diffusion of the primary flow, in the absence of blade row. The behavior of the boundary layer on the blades as well as on the end walls would show a greater tendency to separate, thus increasing the viscous losses, both profile and end wall losses. This is one of the reasons for the deterioration of the rotor performance observed by Schulze et al. in the case of diverging flow. The peak efficiencies measured by Schulze et al. at $A_2/A_1 = 1.15$, 1.00, 0.85 and 0.7 are, respectively, 93, 97.5, 96.5 and 97.5%.

It is clear that the theory devleoped in this paper predicts not only the lift but also the loading coefficient and pressure distributions accurately for $1.0 < VR < 1.25$. It is likely to be accurate for diverging flows, in the absence of viscous effect, for $0.7 < VR < 1.0$. The range, $0.7 < VR < 1.25$, covers the majority of the flows encountered in practice.

## IV. Discussion and Conclusions

It has been established in this paper, both theoretically and experimentally, that the effect of change in mean velocity on the airfoil characteristics is considerable and its effect on

pressure distribution, circulation and lift can be predicted accurately for small change in mean velocity ($0.7 < VR < 1.25$). The expression for vortex distribution, derived in this paper satisfies the kinematic and Kutta conditions exactly. It is found that the ratio of lift coefficients in diverging or converging flow and the two-dimensional value varies linearly with $VR$, i.e.,

$$C_L/C_{L_{2d}} \simeq VR$$

In a converging flow, the circulation and lift increases with increase in velocity ratio (outlet velocity/inlet velocity). There is also considerable change in airfoil pressure distribution, its effect being dominant on the suction surface. In a diverging flow, both the circulation and lift decrease with decrease in velocity ratio. The effect of change in mean velocity on pressure distribution is likely to be dominant on the pressure surface. These changes in the airfoil pressure distribution affect the viscid characteristics of the airfoil, thus adversely affecting the cavitation characteristics of a hydrofoil or pump blade, stall characteristics of a wing, pressure rise characteristics of a fan or compressor blade row. Incorporation of these effects is, thus, a practical necessity.

The pressure distribution measured at midspan and at $Z =$ 3 in. are found to be identical, thus confirming the validity of the quasi two-dimensional approach taken in this paper. The theory is valid exactly at the midspan of the airfoil, where the spanwise velocity is zero, and becomes progressively inaccurate near the converging or diverging walls, where the spanwise velocities cannot be neglected.

## References

[1] Shaalan, M. R. A. and Horlock, J. H., "The Effect of Change in Axial Velocity on the Potential Flow in Cascade," R & M 3547, 1968, Aeronautical Research Council, London, England.

[2] Mani, R. and Acosta, A. J., "Quasi Two-Dimensional Flows Through a Cascade," *Transactions of the ASME*, Vol. 90, No. 2, April 1968.

[3] Wilson, M. B., Mani, R., and Acosta, A. J., "A Note on the Influence of Axial Velocity Ratio on Cascade Performance," *Proceedings of the International Symposium on Fluid Mechanics and Design of Turbomachinery*, The Pennsylvania State University, 1970; also to be published as NASA SP (1).

[4] Lakshminarayana, B., Discussion of Paper by Wilson et al., *Proceedings of the International Symposium on Fluid Mechanics and Design of Turbomachinery*, The Pennsylvania State University, 1970, (to be published as NASA SP).

[5] Erwin, J. R. et al., "Two Dimensional Low Speed Cascade Investigation of NACA Compressor Blade Section Having a Systematic Variation in Mean-Line Loading," TN 3817, Nov. 1956, NACA.

[6] Schulze, W. M., Erwin, J. R., and Ashby, G. C., "NASA 65 Series Compressor Rotor Performance with Varying Annulus Area Ratio, Solidity, Blade Angle and Reynolds Number and Comparison with Cascade Results," TN 4130, Oct. 1957, NACA.

MAY 1972 J. AIRCRAFT VOL. 9, NO. 5

# Methodology for Structural Optimization of STOL Aircraft Vertical Stabilizers

BERTRAM C. WOLLNER*
*Lockheed-California Company, Burbank, Calif.*

**A method is described for selecting the optimum vertical surface configuration for STOL transport configurations, based upon structural weight and performance requirements. A minimization technique, using the Fiacco-McCormick penalty function[1] is used to obtain a solution based upon minimization of an objective function. Design loads for the vertical surface are considered to be defined by the requirement for trim under an engine failure condition. Since structural weight is configuration sensitive, the optimum surface is defined by this condition. Variables include maximum surface deflection and control surface chord ratios. Structural strength requirements are established for a range of configurations typical of STOL aircraft designs. Structural weight is defined in terms of applied load, stabilizer configuration and relevant design parameters. This relation defines an objective function which is minimized in determining the optimum stabilizer configuration based upon structural weight. The system derived is solved using the SLUMT algorithm of Fiacco and McCormick with the Powell direct search technique for constrained nonlinear optimization.[2]**

## Nomenclature

$AR_e$ = vertical stabilizer effective aspect ratio
$AR_v$ = vertical stabilizer aspect ratio
$b$ = span, ft
$c_R$ = vertical stabilizer root chord, ft
$c_T$ = vertical stabilizer tip chord, ft
$c_W$ = wing mean chord, ft
$C_{L_{max}}$ = airplane maximum lift coefficient
$C_{n_\beta}$ = yawing moment derivative per degree sideslip
$C_{n_\delta}$ = yawing moment derivative per degree control surface deflection
$Cy_\beta$ = side force coefficient per degree sideslip
$Cy_\delta$ = side force coefficient per degree control surface deflection
$l_v$ = tail length, ft
$q$ = dynamic pressure, psf
$P_{YVT}$ = total aerodynamic load on vertical stabilizer, lb
$S$ = area, sq. ft
$(T-D)\bar{y}$ = yawing moment due to loss of engine, ft-lb
$W$ = weight, lb

Presented as Paper 71-769 at the AIAA 3rd Aircraft Design and Operations Meeting, Seattle, Wash., July 12–14, 1971; submitted July 23, 1971; revision received January 26, 1972. Appreciation is expressed to G. Smith of San Fernando Valley State College who provided the optimization subroutine used in the study and participated in its implementation.

Index categories: Optimal Structural Design; Aircraft Configuration Design.

* Design Specialist, Senior, Structural Analysis Department. Associate Fellow AIAA.